Open Access

Research Article

PRNANO

Precis. Nanomed. 2020;3(4):710-723

ANDOVER HOUSE

Co-encapsulation by Flash NanoPrecipitation of Insulin, Trypsin Inhibitor and Caprate Permeabilization Enhancer for Oral Administration

Simon A. McManus[1†], Yingyue Zhang[1†], Bumjun Kim[1], Byung Kook Lee[2], Mohamed E.H. ElSayed[2*], Robert K. Prud'homme[1*]

[1.] *Department of Chemical and Biological Engineering, Princeton University, Princeton, New Jersey 08854, United States*

[2.] *Biotechnology Discovery Research, Eli Lilly and Company, Lilly Technology Center North Indianapolis, Indiana 46221, United States*

Submitted: September 21, 2020 Accepted: December 16, 2021 Published: December 19, 2020

Graphical Abstract

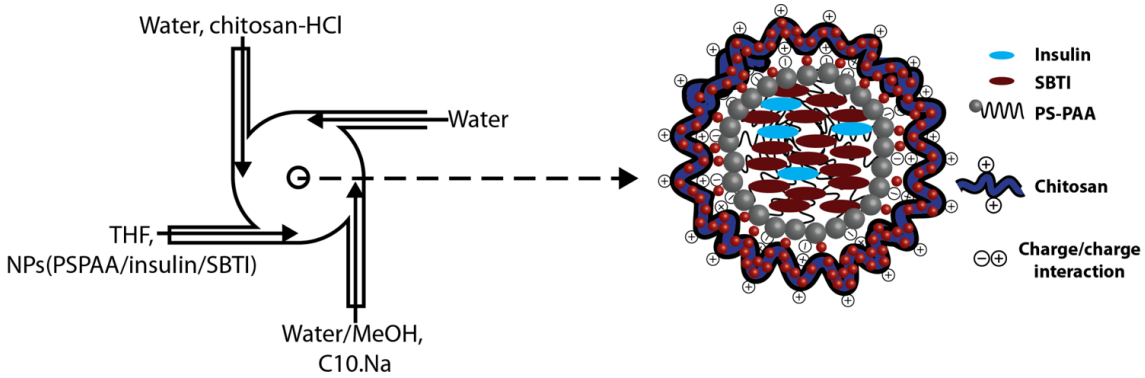

Abstract

We describe inverse-Flash NanoPrecipitation as a new scalable platform for co-encapsulation of insulin (a model therapeutic peptide) with soybean trypsin inhibitor (a peptidase inhibitor) and sodium caprate (a permeation enhancer) forming 300 nm particles for oral delivery. The co-encapsulation of the protein therapeutic with a protease inhibitor and a permeation enhancer into nanoparticles addresses enzymatic attack on the protein drug and the transport across the gastrointestinal tract barrier. Inverse-Flash NanoPrecipitation (iFNP) encompasses two sequential precipitation processes. First, insulin, soybean trypsin inhibitor (SBTI), and hydroxypropyl methylcellulose acetate-succinate polymer (HPMCAS, a stabilizing block copolymer)(at mass ratios of 1:4:5) are rapidly precipitated into an organic antisolvent forming the inverted nano-core (iNC) with 50 wt% insulin and SBTI. Encapsulation efficiencies are greater than 98%. The second step involves the precipitation of sodium caprate and a stabilizing polymer coating onto the iNCs surface. HPMCAS, chitosan, and PEG polymers are used to coat the iNCs to generate nanoparticles with anionic, cationic, and neutral surfaces, respectively. This demonstrates that the iFNP platform can encapsulate complex biologics mixtures at high loadings into particles with customizable surface properties.

Keywords:

Nanoparticle, nanocarrier, insulin, Soybean trypsin inhibitor, SBTI, enzyme inhibitor, caprate, permeabilization enhancer, Flash NanoPrecipitation, inverse Flash NanoPrecipitation, drug delivery

* Robert K. Prud'homme, Department of Chemical and Biological Engineering, Princeton University, Princeton, NJ 08544, Email: prudhomm@princeton.edu, Phone: +1-(609) 258-4577, and Mohamed E.H. ElSayed, Ph.D., E-mail: Mohamed.elsayed@lilly.com, Phone: +1 (317) 277-4696

Prnano.com, https://doi.org/10.33218/001c.18519
The official Journal of CLINAM – ISSN:2639-9431 (online)

Rationale and Purpose

Peptide and protein therapeutics are the fastest-growing segments of the pharmaceutical market. Their greater specificity and lower non-specific toxicity compared with small molecule drugs have driven this growth [1, 2]. However, the greatest challenge in the field is delivery. Although there have been significant advances, oral delivery is still a mostly unrealized opportunity [3]. Complex processing strategies for encapsulation and limitations on the biologic loading and loading efficiency have slowed clinical translation. Typical liposome loadings are at most 10 wt%, while polymeric nanocarriers are frequently 2 wt% or less [4-12].

Introduction

We present a new encapsulation approach that addresses these limitations. The technique termed inverse-Flash NanoPrecipitation (iFNP) is a two-step encapsulation process. In the first step, the soluble biologic precipitates as a block-copolymer protected nanoparticle into a non-aqueous phase. Subsequently, a second step provides a biocompatible coating layer. Figure 1 shows the concept map for the nanocarrier constructs that can be prepared by iFNP.

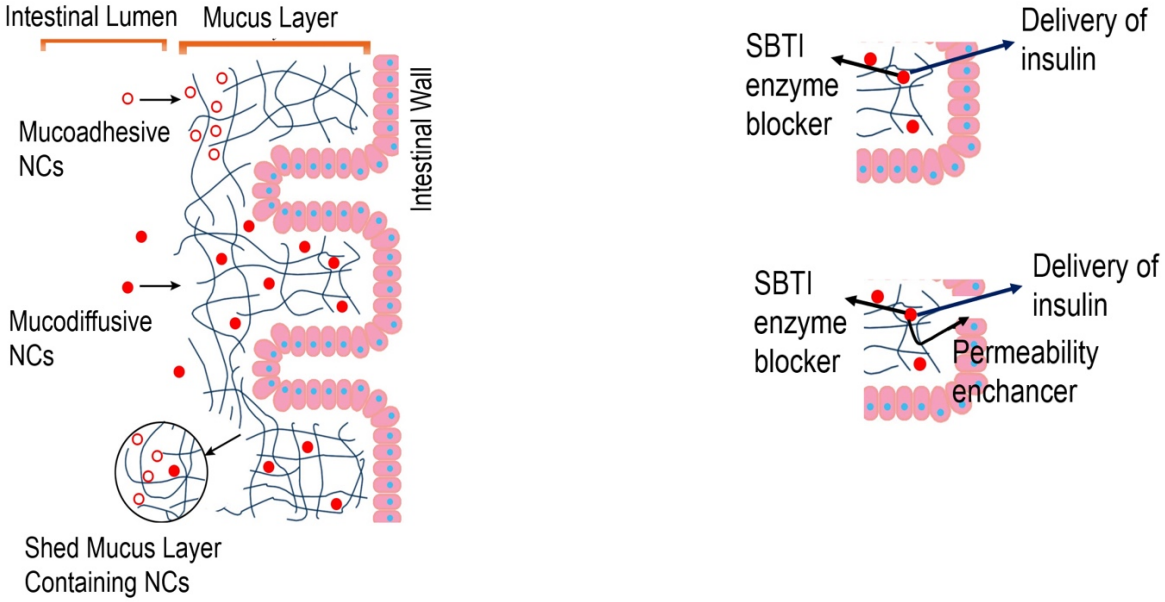

Figure 1. Concept map of nanocarrier (NC) delivery of insulin. The schematic shows the two concepts. A) NCs may be mucoadhesive or muco-diffusive. B) NCs may release an enzyme inhibitor (SBTI) to prevent protein degradation, and the protein, or the NCs may release an enzyme inhibitor, the protein, and a permeabilization enhancer to increase delivery effectiveness.

The first step creates highly loaded cores (50 wt% biologic) at 98% encapsulation efficiency. In the second coating step, neutral (PEG), anionic, or cationic coatings are assembled on the nanoparticle surface. Both steps involve a continuous, block-copolymer-directed, kinetically controlled precipitation under turbulent flow in specially designed mixing chambers [13-15]. The block-copolymer precipitation process is scalable – the same 100 nm nanoparticles have been demonstrated using 1 mg of sample and at 10 L/minute to make 300 L batches [16]. The previous examples of the iFNP process [12, 17, 18] have been directed to parenteral administration and do not present the challenges associated with oral protein delivery. To address oral delivery, the peptides/proteins are formulated with peptidase inhibitors to minimize the degradative effect of GIT enzymes and permeation enhancers to increase peptide's diffusion across the epithelial barrier. There is debate about whether oral deliv-

Prnano.com, https://doi.org/10.33218/001c.18519
The official Journal of CLINAM – ISSN:2639-9431 (online)
Andover House, Andover, MA USA

ery of nanoparticles is best achieved when the nanoparticles' surfaces are mucoadhesive [19, 20] or when they are neutral (PEG) and mucodiffusive [21, 22]. Therefore, to demonstrate the iFNP platform's flexibility, we prepare nanoparticles with highly cationic, anionic, and neutral surfaces. The nanocarriers (NCs) can be prepared with surface coatings to make them mucoadhesive or mucodiffusive, and the NCs can encapsulate insulin, a protease inhibitor (SBTI), and a permeabilization enhancer (sodium caprate).

Materials and Methods

Experimental Design

The goal of this proof-of-concept study was to evaluate the ability of the iFNP process as a robust and scalable platform for encapsulation of complex mixtures of therapeutic peptides and functional excipients into nanoparticles (NPs) with tunable surface charge to facilitate specific interactions with the mucus lining of the intestinal tract. Insulin was chosen as the model peptide, while soybean trypsin inhibitor (SBTI, 21 kDa) was used as a peptidase inhibitor to minimize insulin degradation in the GI tract, and sodium caprate (C10) was chosen as a permeation enhancer. The first step of iFNP involved the precipitation of insulin and SBTI. For this model study, a non-degradable polystyrene-b-polyacrylic acid (PS-b-PAA) was used as the stabilizing polymer for the inverted nano-core (iNC). Hydroxypropyl methylcellulose acetate-succinate polymer (HPMCAS 126), chitosan and polyethylene glycol (PEG) polymers were used in the second precipitation step to generate anionic, cationic and neutral NPs, respectively.

Materials.

Soybean trypsin inhibitor (SBTI) and zinc chloride were purchased from Sigma Aldrich. Insulin-Zn was supplied by Eli Lilly and Company. Polystyrene-block-polyacrylic acid (PS_{5k}-b-$PAA_{4.8k}$) polystyrene-block-polyethylene glycol ($PS_{1.6k}$-b-PEG_{5k}) was purchased from Polymer Source (Dorval Canada). The non-degradable block copolymer was chosen to achieve particle formation without involving polymer hydrolysis, as would occur for polylactide-based polymers. However, we have shown that self-assembly works equally well with biodegradable polymers.[18, 23] HPMCAS 126 was supplied by Dow Chemical Company. Chitosan (90%+ deacetylated) was purchased from Spectrum Chemicals (New Brunswick, NJ). All solvents were purchased from Fisher Scientific.

Inverse Flash NanoPrecipitation (iFNP).

iFNP was performed using a confined impinging jet mixer (CIJ) by rapidly mixing a solvent stream (95% DMSO, 5% water) against an antisolvent (DCM) stream. The operation and design of the mixer have been described previously [17]. Two syringes were used to inject 500 µL of the solvent and 500 µL of antisolvent through the CIJ mixer. When using the four-jet multiple inlet vortex mixer (MIVM) mixer, four 500 µL syringes were used. The solvent stream contained PS_{5k}-b-$PAA_{4.8k}$ and insulin and/or SBTI at desire ratios. For example, an iFNP experiment encapsulating insulin and SBTI was carried out as follows. PS-b-PAA and insulin were dissolved separately in DMSO. SBTI was dissolved in water at 20× of the desired final concentration. Polymer and peptides were mixed and diluted with DMSO such that the final solvent mixture contained 95% DMSO and 5% water with final concentrations of 5 mg/mL PS-b-PAA, 4 mg/mL SBTI, and 1 mg/mL insulin. In experiments with only insulin or SBTI, the remaining volume was made up with water or DMSO. Zinc chloride was dissolved in methanol and added to the DCM antisolvent stream affording a 1:1 charge ratio accounting for the total negative charge contributed by PS-b-PAA. Typically, 0.5 mL of solvent stream was impinged against 0.5 mL of antisolvent using a CIJ mixer and diluted into a reservoir of 4.5 mL of additional antisolvent.

Extraction of DMSO and Transfer of Inverse Nano-Cores (iNCs) from DCM to Water-Miscible Solvents.

DMSO was extracted from the iNC dispersion after iFNP. To 5 mL of iNCs, 3 mL of either brine (13% w/w NaCl) or 1× phosphate-buffered saline (PBS) was added, and the mixtures were gently shaken on a tabletop shaker for 30 minutes. Samples were transferred to 15 mL conical tubes and centrifuged using a bucket rotor at 2000 RCF for 5 minutes at room temperature. DCM phase on

Prnano.com, https://doi.org/10.33218/001c.18519
The official Journal of CLINAM – ISSN:2639-9431 (online)
Andover House, Andover, MA USA

the bottom was carefully transferred and iNC size post-DMSO extraction was measured via DLS. iNCs were transferred from DCM to a water-miscible solvent by repeated rounds of concentration and dilution. 4 mL of tetrahydrofuran (THF) or acetone was added to 5 mL of extracted iNCs. This iNC suspension was concentrated by rotary evaporation to 1 mL. Seven mL of THF or acetone was then added, and the mixture was again concentrated to 1 mL. Two additional rounds of dilution and concentration were performed, leading to a final suspension of iNCs in 1 mL of THF or acetone.

FNP of iNCs with HPMCAS 126, chitosan, or PEG.

iNCs were coated with HPMCAS, chitosan, or PEG by FNP. For all experiments, the mass ratio of coating polymer to iNCs was kept constant at 1.5:1. The coating polymers and mixing conditions for each are described in the Results and Discussion section. The coating polymer was first dissolved in THF and added to concentrated iNCs in THF. This mixture was impinged against water at a 1:1 volume ratio in a CIJ mixer and immediately diluted 9x further in water.

Encapsulation Assays.

Encapsulation efficiency (EE) and release were evaluated by high-performance liquid chromatography (HPLC). After the second coating was added by FNP and THF, for EE measurements, samples were removed under vacuum and were passed through a wetted 100 kDa Amicon® filter. The filtrate was lyophilized and resuspended in 1/10 its original volume for better detection by HPLC. Standard curves for insulin and SBTI (provided in Supplemental Information (SI)) were developed with UV−vis spectrophotometry at 210 nm. The unencapsulated insulin and SBTI was less than 10% of the amount loaded in all samples, meaning that the EE was 90+%. With the non-degradable PS-b-PEG polymer used for the initial iFNP step, it was impossible to solubilize and release the iNC components to measure EE on the iNCs directly, rather than measuring the unencapsulated components. The overall processes involved in the study are schematically shown in Figure 2.

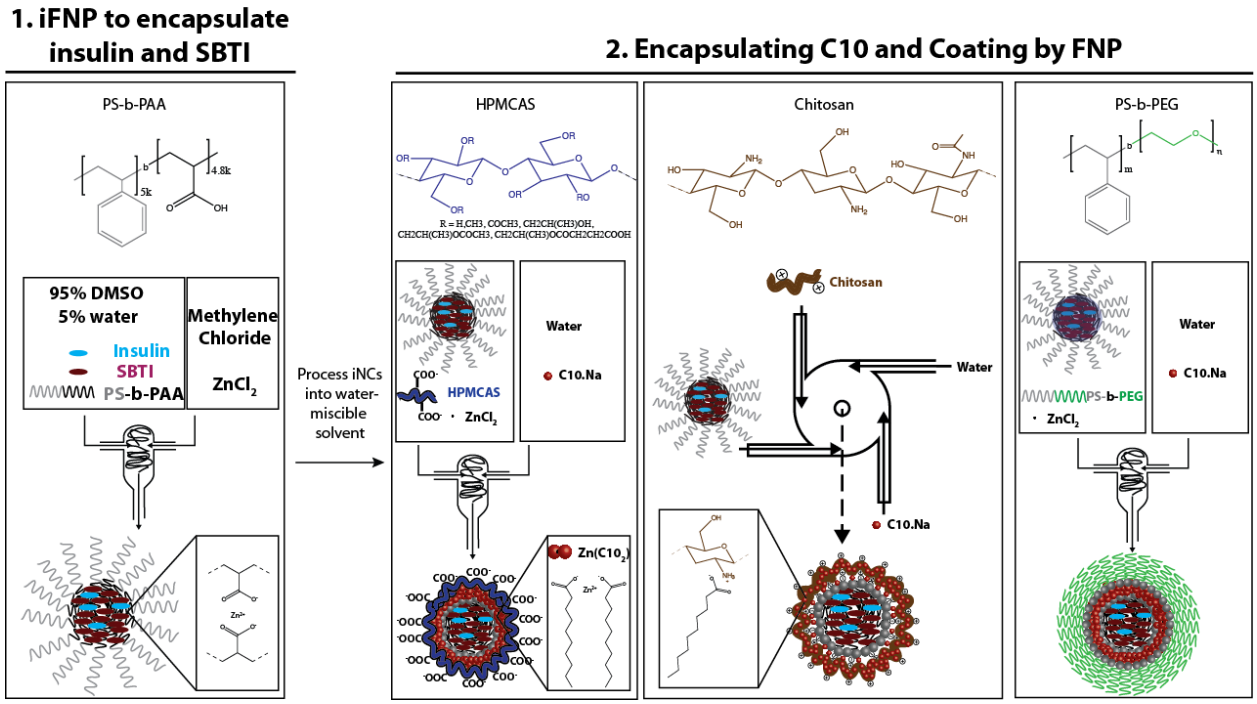

Figure 2. General Scheme for Encapsulation of Insulin, SBTI, and C10 into Nanoparticles . 1. Inverse Flash NanoPrecipitation (iFNP) to encapsulate insulin and SBTI. 2. Flash NanoPrecipitation (FNP) to encapsulate C10 and coat with HPMCAS, chitosan, or polyethylene glycol (PEG)

Prnano.com, https://doi.org/10.33218/001c.18519
The official Journal of CLINAM – ISSN:2639-9431 (online)
Andover House, Andover, MA USA

Dynamic Light Scattering (DLS) and Zeta Potential.

Particle size and zeta potential measurements were taken using a Malvern Nano ZS equilibrated at 25˚C. For DLS measurements, samples were diluted 10-fold in a matching solvent and measured at a scattering angle of 173 degrees with a 632 nm helium-neon laser. The reported sizes shown were the mean of three measurements of 10 runs each. Reported Z-average diameters are the intensity-weighted diameters obtained from DLS measurements, and PDI is the polydispersity index obtained from the cumulants fitting program and reported by the DLS instrument. For zeta potential measurements, samples were diluted with 1× PBS, to a final concentration of 0.1× PBS. Zeta potential measurements were carried out using zeta potential mode and the Smoluchowski model. The detailed size and PDI results of nanoparticles could be found in SI.

Results and Discussion

Encapsulation of SBTI and Insulin by Inverse Flash NanoPrecipitation (iFNP):

In the first step, the insulin and SBTI were encapsulated using iFNP. The term "inverse" denotes that a water-soluble species is being precipitated into an organic phase, in contrast to the normal FNP that involves precipitating hydrophobic species into water [12, 24, 25]. The principles of operation of the mixers using in FNP and iFNP processing CIJ have been described previously [13-15]. SBTI, insulin, and PS-b-PAA were solubilized in DI water and DMSO with a final solution comprising 95% DMSO/5% water. The optimal ratio of insulin to SBTI had been selected as 1:4 by mass. This solution was then micro-mixed against a solution of $ZnCl_2$ in DCM as antisolvent using a CIJ mixer. The Zn^{2+} ionically crosslinked the block copolymer's free carboxylic group and stabilized the inverted nano-cores (iNCs) for the subsequent coating step. iFNP produced PS-PAA iNCs of 49±2 nm for the insulin alone, 74± 2 nm for SBTI alone, and 82± 2 nm for the combined insulin and SBTI, as shown in Figure 3B. In the first iFNP step, the combined insulin and SBTI iNCs comprised 50 wt% protein. The strength of crosslinking was evaluated by testing the swelling of the NCs in 90% DMSO, with the retention of iNC size indicating substantial crosslinking [18]. Without Zn^{2+} as the crosslinker, iNCs dissolved in DMSO (data not shown).

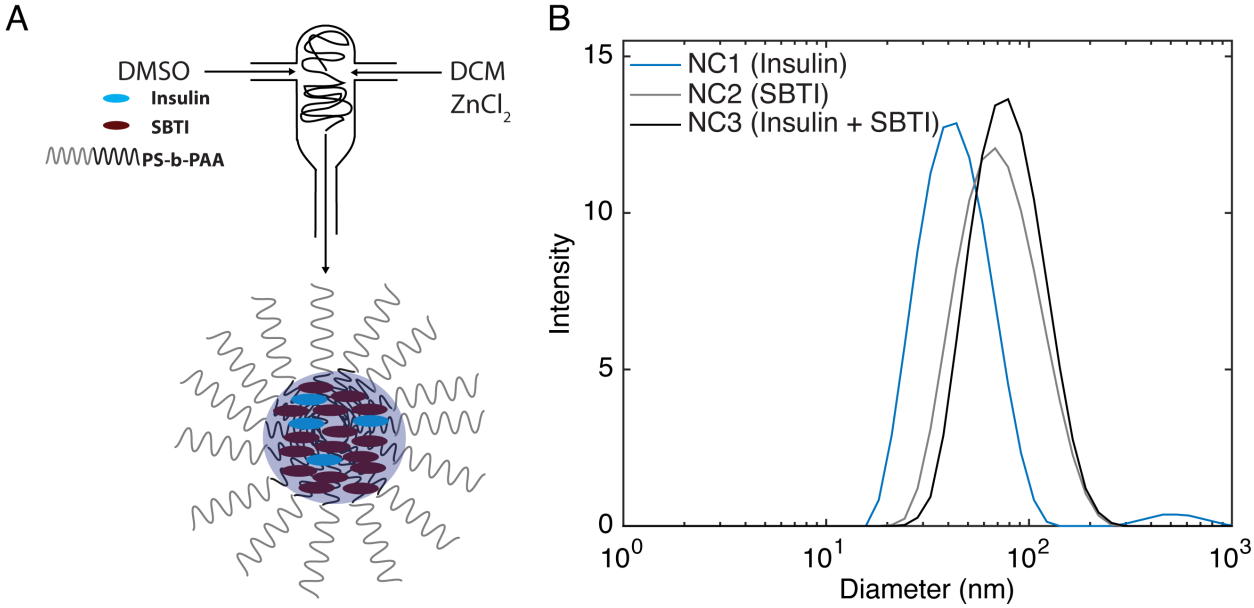

Figure 3: Encapsulation of insulin and SBTI by iFNP. A) Schematic of the iFNP process used to encapsulate insulin and SBTI. B) iNC size distribution by DLS of PS-PAA/insulin (49nm), PS-PAA/SBTI (74nm), and PS-PAA/insulin/SBTI (82nm) produced by iFNP. The detailed size and PDI results are provided in SI.

Prnano.com, https://doi.org/10.33218/001c.18519
The official Journal of CLINAM – ISSN:2639-9431 (online)
Andover House, Andover, MA USA

Transferring iNCs into Water-Miscible Solvent and Extraction of DMSO.

The iNCs made with PS-b-PAA/insulin/SBTI in DCM were first extracted to remove DMSO and then transferred into a water-miscible solvent to enable the next FNP coating step. Comparing size distributions before and after extraction in Figure 4A demonstrated that the iNC remained at its initial size after extraction of DMSO by either NaCl or PBS.

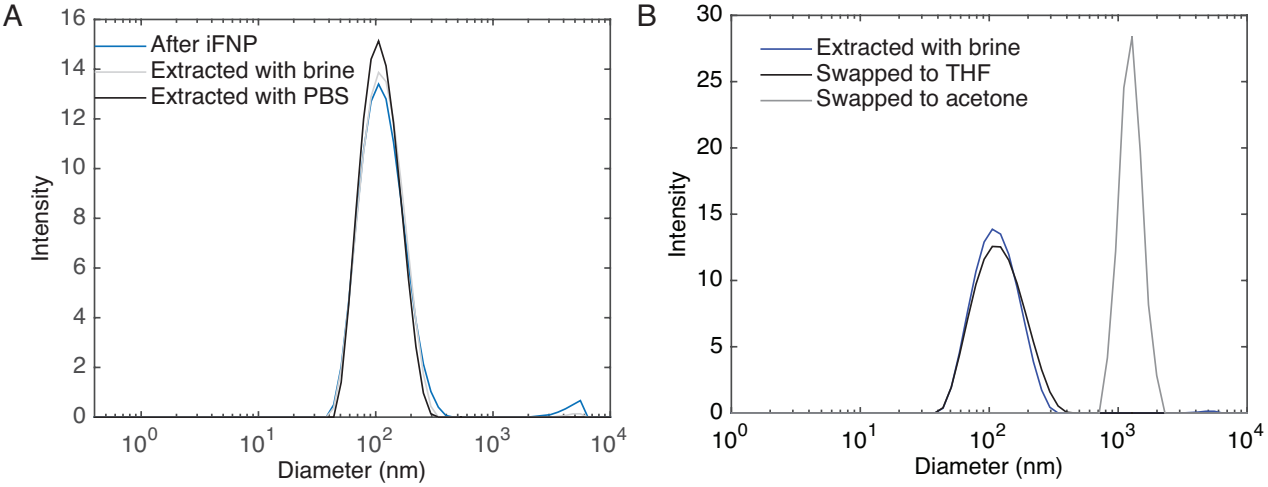

Figure 4: Processing of iNC to remove DMSO and solvent swapping into water-miscible solvents. A) Extraction with either NaCl or PBS produced no change in NCs sizes. B) Solvent swapping into THF caused no change in NCs size; however, exchanging into acetone resulted in NCs aggregation because the external PS steric stabilizing layer is not sufficiently soluble in acetone. The detailed size and PDI results are provided in SI.

To transfer the iNCs to a water-miscible solvent for the second coating step, iNCs were solvent swapped into THF or acetone using a rotary evaporator. Figure 4B shows that after swapping into THF, iNCs size distribution remained the same as before solvent swapping. When swapped into acetone, the iNCs average size increased from 105 nm to a few µm due to particle aggregation in this solvent. This indicated that the PS steric stabilizing coating on the iNCs were not sufficiently soluble in acetone; consequently, the iNCs aggregated. All further experiments were conducted in THF.

Anionic Surface Functionalization: HPMCAS.

The NCs, now in a water-miscible organic solvent, must be coated with a biocompatible surface stabilizer and transferred into an aqueous phase. This is accomplished with a second FNP step. iNCs were covered with HPMCAS, where the carboxylic acids provide the anionic charge, as shown in Figure 5A. HPMCAS at a 1.5 mass equivalent (relative to iNCs mass) was mixed with iNCs in THF. This mixture was flash precipitated against water using a CIJ mixer and immediately diluted 9× with water. NCs size distributions are shown in Figure 5B.

The initial iNC diameter was 214 nm, upon coating the final nanoparticles (NPs) size was 322 nm. The increase in size is consistent with a diffuse HPMCAS surface layer of 54 nm. It is known that HPMCAS creates gels that slowly hydrate and erode in sustained-release tablets. However, during the rapid FNP precipitation process, the hydrophobic acetyl groups anchor on the hydrophobic NC surface, and the carboxylic acid groups orient into the solvent phase to form colloidally stable NPs, rather than aggregated gels. The electrostatic repulsion between particles prevents aggregation and creates the stabilized NPs shown in Figure 5.

Prnano.com, https://doi.org/10.33218/001c.18519
The official Journal of CLINAM – ISSN:2639-9431 (online)
Andover House, Andover, MA USA

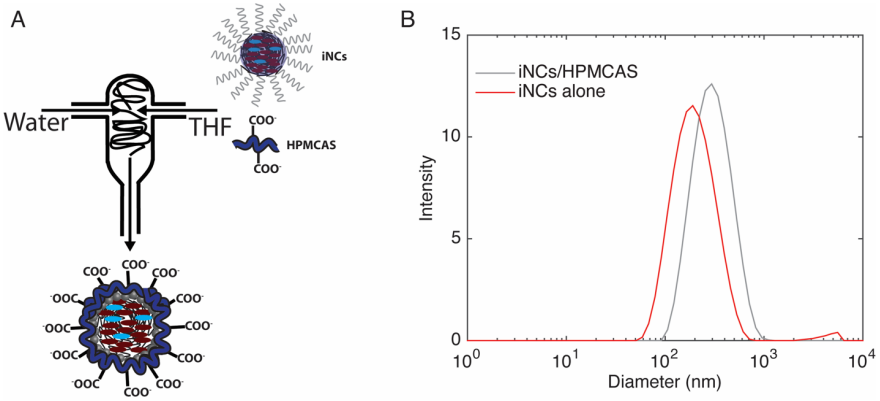

Components	Size (nm)	PDI
iNCs/HPMCAS	322 ± 6	0.18
iNCs alone	214 ± 5	0.27

Figure 5: iNC Coating with HPMCAS. (A) iNCs swapped into THF were coated with HPMCAS 126G in a second FNP step. (B) The initial size distributions of the iNCs in DCM and the HPMCAS coated iNCs are shown.

Cationic Surface Functionalization: Chitosan:

Two approaches were used to deposit the cationic chitosan on the iNC surfaces using FNP. In each case, the chitosan was introduced in the aqueous phase, and the iNCs were introduced in the THF phase. The difference was the cationic charge on the chitosan. In the first case, chitosan was dissolved in 1% aqueous acetic acid to ionize the amine groups and mixed with a CIJ mixer against iNCs in THF. The dispersion was immediately diluted with 9x water by volume. The NCs aggregated to ~1 micron. The acetic acid did not sufficiently ionize the chitosan to produce electrostatic repulsions strong enough to prevent aggregation. In contrast, when chitosan was isolated from a strong acid solution as an amine:HCl and the chitosan:HCl was dissolved in water and put through the same FNP process, 321 nm stable NPs were produced. The DLS data in Figure. 6B shows that the chitosan layer was 80 nm thick, indicating a diffuse steric layer on the NCs surface.

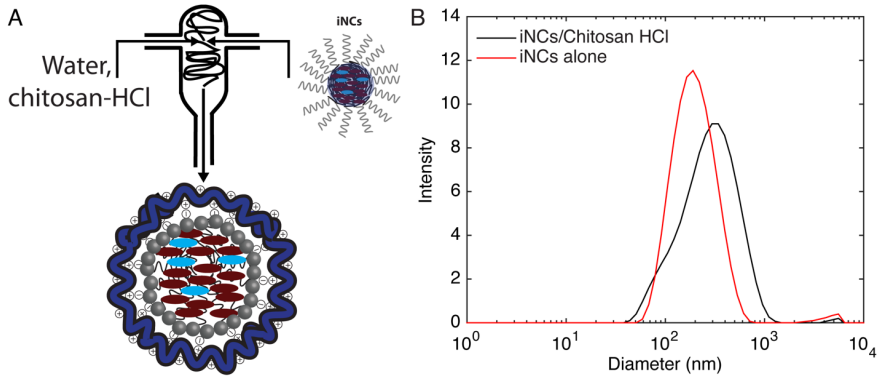

Components	Size (nm)	PDI
iNCs/Chitosan.HCl	321 ± 17	0.28
iNCs alone	161 ± 4	0.27

Figure 6: Coating iNCs with chitosan-HCl. (A) Schematic of FNP process, (B) DLS data on initial iNCs in DCM and final size distribution after chitosan surface functionalization.

Prnano.com, https://doi.org/10.33218/001c.18519
The official Journal of CLINAM – ISSN:2639-9431 (online)
Andover House, Andover, MA USA

Neutral Surface Functionalization: PEG:

For a neutral surface, $PS_{1.6k}$-b-PEG_{5k} was deposited using FNP. PS-b-PEG was added to the iNCs in THF and flashed against an equal volume of water, followed by immediate dilution in 9x water. The resulting NPs were 172 nm in size. The DLS data in Figure. 7 shows a small PS-b-PEG micelle peak at ~30 nm and then a prominent NP peak.

.

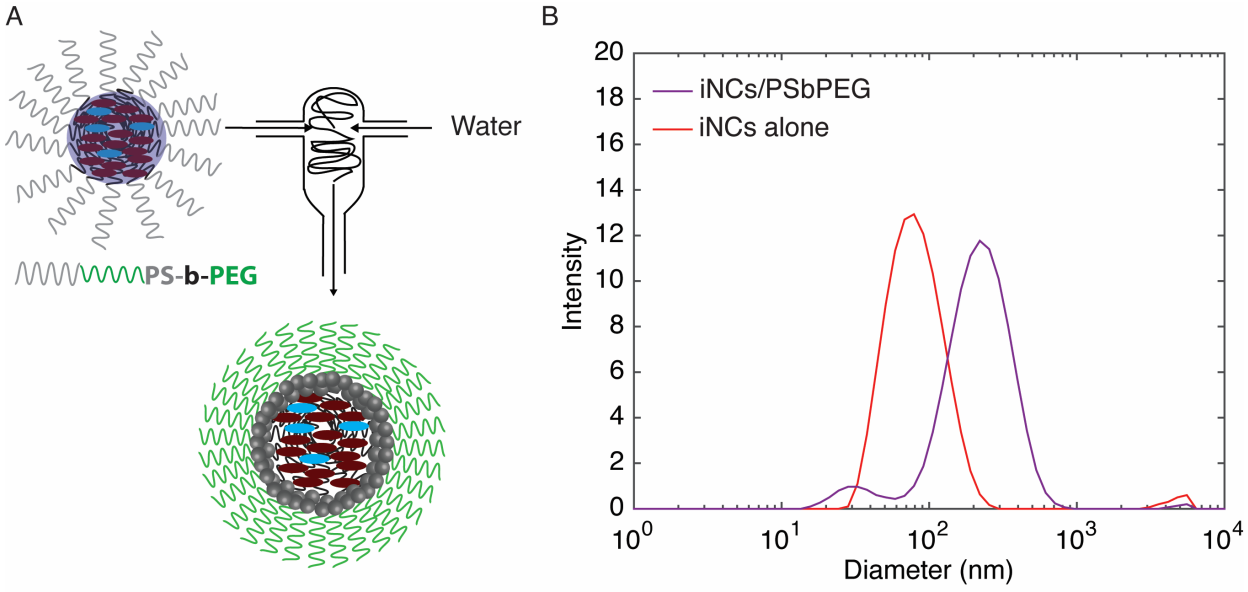

Components	Size (nm)	PDI
iNCs, PS-b-PEG	172 ± 8	0.56
iNCs alone	88 ± 4	0.19

Figure 7. iNC Coating with PS-b-PEG. (A) iNCs swapped into THF were coated with PS-b-PEG in a second FNP step. (B) The size distributions of the iNCs in DCM, transferred to THF, and coated with PS-b-PEG are shown. The sizes increase upon coating with the PS-b-PEG layer to 172 nm.

The increase in size by 84 nm is larger than expected for the PS-b-PEG layer alone, which should increase in size approximately equal to that of the micelle size (i.e., ~ 30 nm). Micelles of this size can be readily removed from the large NP population by ultrafiltration. The PS-b-PEG corona size has been studied and modeled by Pagels [23]. The increase in size might result from some loss of stability, and limited aggregation, as some of the stabilizing polymer is lost due to micellization.

Incorporation of Caprate (C10) Permeabilizing Agent:

The formulation's final element requires co-encapsulation of sodium caprate (C10) in the NPs with the insulin/STBI. The mass ratio of caprate to insulin was chosen to be 4:1 in all of the NC formulations. Different mechanisms are required to incorporate the caprate in the anionic HPMCAS NCs, the cationic chitosan NCs, and the neutral PS-b-PEG NCs. The HPMCAS polymer is significantly hydrophobic and will bind with hydrophobic compounds. We transformed the anionic caprate into a hydrophobic complex by combining it with $ZnCl_2$. FNP was performed with sodium caprate dissolved in water impinged against HPMCAS, iNCs, and $ZnCl_2$. $ZnCl_2$ interacts ionically with C10 to form a hydrophobic $ZnC1_2$ complex that can be incorporated into the hydrophobic layer of the HPMCAS coated iNCs. The ratio of C10 to $ZnCl_2$ was chosen as 2:1 on a charge equivalent basis.

Prnano.com, https://doi.org/10.33218/001c.18519
The official Journal of CLINAM – ISSN:2639-9431 (online)
Andover House, Andover, MA USA

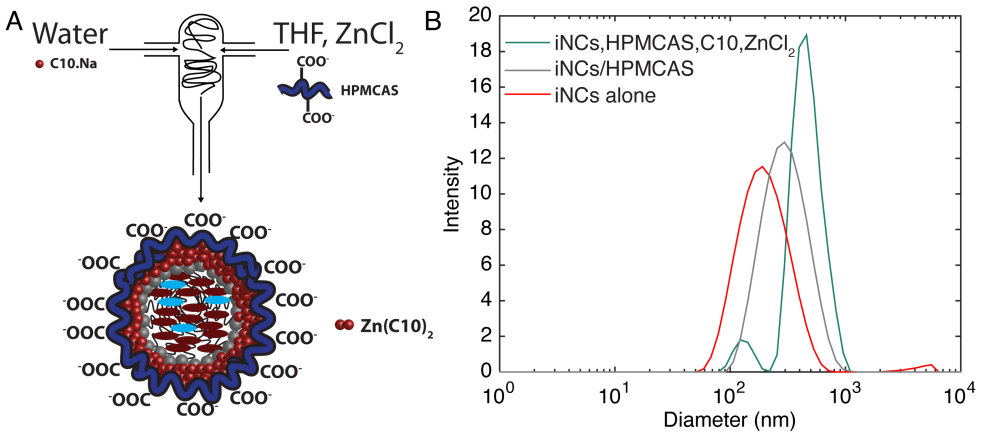

Components	Sizes (nm)	PDI
iNCs/HPMCAS/Zn/C10	486 ± 60	0.40
iNCs/HPMCAS	322 ± 6	0.18
iNCs alone	214 ± 5	0.27

Figure 8: Coating with HPMCAS and sodium caprate (C10) permeation enhancer . To incorporate C10 into the hydrophobic layer of HPMCAS-coated NPs , FNP was performed with sodium caprate dissolved in water impinged against HPMCAS, iNCs, and ZnCl2. The initial 214 nm size is increased to 486 nm by the C10 inclusion.

Figure 8 shows the iNC coated with HPMCAS alone, which produced NCs of 322 nm. When C10:$ZnCl_2$ was added to the formulation, the resulting NCs were 486 nm. There is a main peak and a smaller peak at ~100nm, which may be C10:$ZnCl_2$ encapsulated by hydroxypropyl methylcellulose acetate succinate (HMPCAS) without the core. We have observed previously the formation of larger "coated" nanoparticles that include some of the smaller hydrophobic species and a population of smaller nanoparticles comprising only the smaller hydrophobic species [26].

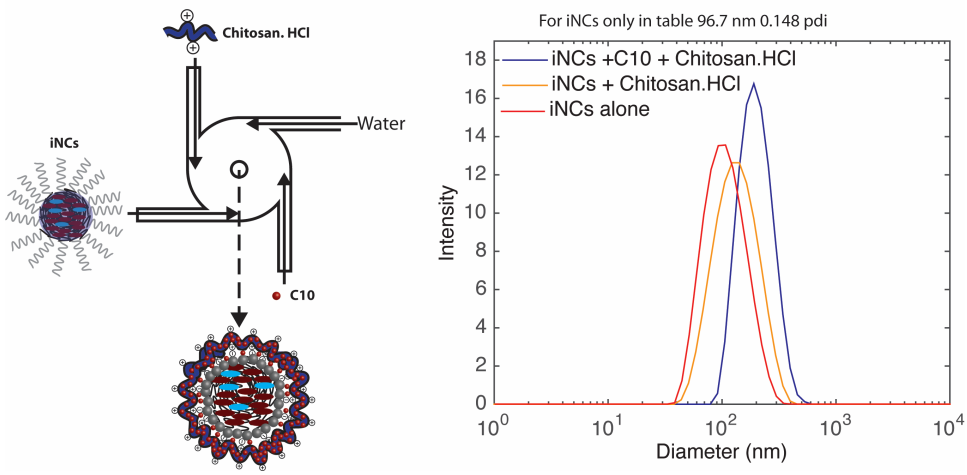

Components	Size (nm)	PDI
iNCs, C10, Chitosan.HCl	206± 7	0.15
iNCs, Chitosan.HCl	143 ± 1	0.17
iNCs alone	96.7 ± 0.7	0.148

Fig. 9. Caprate is complexed with the cationic chitosan NCs via charge interactions. The narrow size distribution at 206 nm indicates successful high loading with the caprate.

Prnano.com, https://doi.org/10.33218/001c.18519
The official Journal of CLINAM – ISSN:2639-9431 (online)
Andover House, Andover, MA USA

In the desired oral application, the delivery of caprate via the 100 nm nanoparticles may be advantageous. The size difference between the 486 nm coated nanoparticles, and the 100 nm nanoparticles would make a centrifugal separation straightforward

The chitosan NCs do not require the Zn salt formation since the anionic caprate can complex with the cationic groups on chitosan (see supplementary Figure S4). The scheme in Figure 9 depicts coating of iNCs with chitosan complexed to C10. To allow complexation of C10 and chitosan to coincide with chitosan interaction with iNCs, a MIVM was used with sodium caprate dissolved in water in one stream, chitosan-HCl dissolved in water in a second stream, a third stream of water, and a fourth stream of iNCs in THF. If the chitosan and sodium caprate were added to the same aqueous stream, they precipitate and no longer interact with the iNCs in the THF stream. This is an example of the MIVM mixer's flexibility, enabling the assembly of more complex NC formulations. As shown in Figure 9, without C10, the NPs were 143 nm, and with C10 encapsulation, the size increased to 206 nm, demonstrating the co-loading of the C10 into the final NPs. The zeta potential of the chitosan-coated iNCs with C10 was +8 mV (SI Figure S5). The zeta potential of chitosan-coated NCs without C10 is +30 mV, and our previous work on PEG-coated iNCs showed zeta potentials in the range −2 mV - −12 mV [18].

C10 was incorporated into the PS-b-PEG formulation similarly as with the HPMCAS-coating; that is, the hydrophobicity of the C10:$ZnCl_2$ complex was exploited to co-precipitate the complex with the PS hydrophobic blocks of the steric stabilizing polymer.

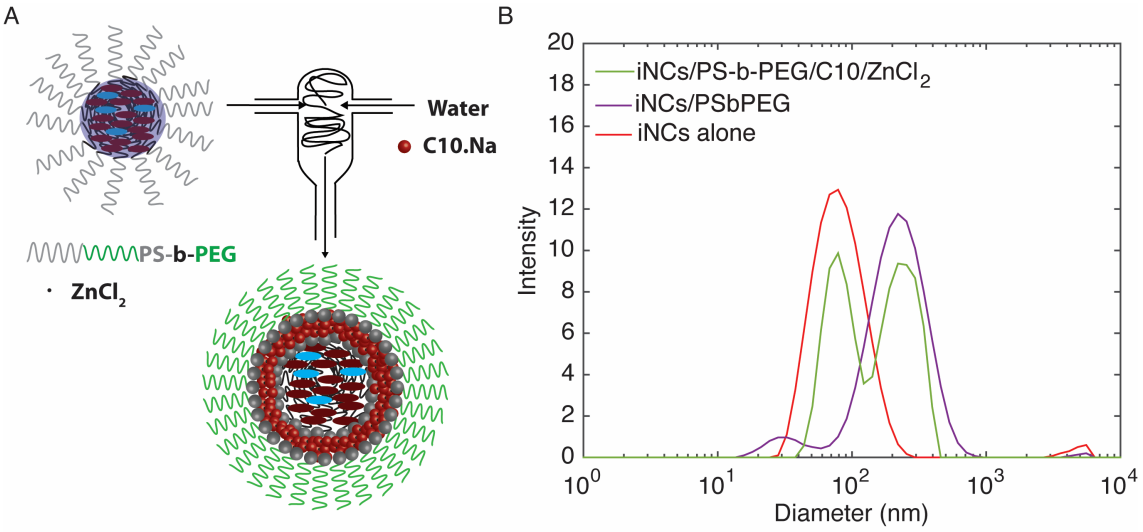

Components	Sizes (nm)	PDI
iNCs/PS-b-PEG/C10/Zn	362 ± 77	0.48
iNCs/PS-b-PEG	172 ± 8	0.56
iNCs alone	88 ± 4	0.19

Figure 10. Coating with PS-b-PEG and caprate permeabilizer. To incorporate the C10 into the hydrophobic layer of PS-b-PEG-coated iNCs, FNP was performed with C10 dissolved in water impinged against PS-b-PEG, iNCs, and $ZnCl_2$. The initial 88 nm size is increased to 362 nm with the caprate inclusion, with a second smaller population observed at 78 nm.

As shown in Figure 10, the NPs size was 360 nm, with a smaller peak at 78 nm. The smaller peak is consistent with block copolymer encapsulation of the C10: $ZnCl_2$ into some NPs, which do not contain the insulin/SBTI cores.

The summary of the formulation conditions for the initial inverse nanocarrier core (iNC) and the finally formulated NC are show in Table 1 and 2, respectively.

Prnano.com, https://doi.org/10.33218/001c.18519
The official Journal of CLINAM – ISSN:2639-9431 (online)
Andover House, Andover, MA USA

Table 1. Formulation conditions for preparation of the initial inverse nanocarriers, iNC

Inverse Nanocarrier Formulation (iFNC)	Stream 1 in CIJ mixer (polar phase with actives: 95vol% DMSO, 5 vol% DI Water)		Stream 2 in CIJ mixer (antisolvent phase: methylene chloride)	
	Concentration	Mass in 500 µL injection	Concentration	Mass in 500 µL injection
Insulin	1 mg/mL	0.5 mg		
Soybean trypsin inhibitor (SBTI)	4 mg/mL	2.0 mg		
PS-b-PAA polymer stabilizer	5 mg/mL	2.5 mg		
$ZnCl_2$ crosslinker			4.62 mg/mL	2.31 mg
	1 mL iFNC from mixer is diluted into 4.0 mL methylene chloride			

Table 2. Formulation for the final coated nanocarriers

Coating Formulation	Stream 1 (THF) Polymer Coating at 1.5:1 mass ratio polymer:iNC		Stream 2 (Aqueous antisolvent)		Stream 3 in MIVM mixer (Aqueous antisolvent)		Stream 4 in MIVM mixer (Aqueous antisolvent)
	Concentration	Mass in 500 µL injection	Concentration	Mass in 500 µL injection	Concentration	Mass in 500 µL injection	
HPMCAS 126	iNC: 10 mg/mL HPMCAS: 15 mg/mL ZnCl2: 2.8 mg/mL	5 mg 7.5 mg 1.4 mg	NaC10: 4 mg/mL	2 mg			
Chitosan	iNC: 10 mg/mL	5 mg	C10: 4.0 mg/mL	2 mg	Chitosan: 15 mg/mL	7.5 mg	500 µL DI water
PEG-b-PS	iNC: 10 mg/ml PEG-b-PS: 15 mg/mL $ZnCl_2$: 2.8 mg/mL	5 mg 7.5 mg 1.4 mg	C10: 4.0 mg/mL	2 mg			
	1 mL iFNC from mixer is diluted into 9 mL DI water for two stream operation						

Prnano.com, https://doi.org/10.33218/001c.18519
The official Journal of CLINAM – ISSN:2639-9431 (online)
Andover House, Andover, MA USA

Inverse nanocarriers (iNCs) are given three separate polymer coatings to prepare negative NCs (HMCAS), cationic (chitosan), and neutral (PEG) surfaces. For those formulations containing the permeabilization enhancer sodium caprate the compositions are presented. For formulations not containing C10 that component was omitted. The HPMCAS and PEG-b-PS coating were applied in a two-stream CIJ mixer and the compositions of those streams are shown. For the HPMCAS and PEG coatings, $ZnCl_2$ was incorporated to precipitate C10 onto the iNC surface. For the chitosan surface, the electrostatic interaction between the chitosan and sodium caprate was used to incorporate the C10. For chitosan coating, the four-stream MIVM was used to prevent the chitosan interacting with the negatively charged C10 anion before mixing.

Conclusions

The results presented show the successful preparation of highly loaded NPs with insulin, trypsin inhibitor, and permeation enhancer. The NPs have been produced by a scalable, facile process involving two precipitation steps using the FNP technology. NPs prepared by this two-step iFNP process demonstrate the feasibility of generating highly loaded nanoparticles encapsulating a mixture of API and functional excipients. We have shown the ability to formulate nanoparticles containing dual protein cores and a hydrophobic excipient (the permeabilization agent, caprate). The flexibility of the processing enables the application of anionic, cationic and neutral surface coatings. In this proof-of-principle study, iNCs were developed using PS-b-PAA, which is a non-degradable polymer. To enable this successful clinical translation of these NPs, biodegradable block copolymers such as polyaspartic acid-b-polylactic acid (PAsp-b-PLA) can be used in the 1st precipitation step to generate the nano-cores [17]. Further, optimization of polymer composition provides an opportunity for controlling the release kinetics of the API and associated excipients.

It is important to note that the iFNP process can be easily interfaced with spray drying or lyophilization to isolate the formulated particles as solids for oral solid dosage formulations. We have demonstrated drying and redispersion to nanoparticle form for similar FNP formulations [27-29]. This study was directed towards addressing challenges in oral peptide delivery; however, these particles also offer interesting opportunities for parenteral administration.

Acknowledgment

We would like to thank Eli Lilly and Company for financial support of this research.

Conflict of Interests

The authors declare no conflicts of interest. For a signed statement, please contact the journal office: editor@precisionnanomedicine.com

Quote this article as: McManus SA, Zhang YG, Kim B, Lee BK, ElSayed MEH, Prud'homme RK, Co-encapsulation by Flash NanoPrecipitation of Insulin, Trypsin Inhibitor and Caprate Permeabilization Enhancer for Oral Administration, Precis. Nanomed. 2020;3(5):710-723, https://doi.org/10.33218/001c.18519

References

[1] H. A. D. Lagassé et al., "Recent advances in (therapeutic protein) drug development," (in Eng), F1000Research, vol. 6, pp. 113-113, 2017.

[2] B. J. Bruno, G. D. Miller, and C. S. Lim, "Basics and recent advances in peptide and protein drug delivery," (in eng), Therapeutic delivery, vol. 4, no. 11, pp. 1443-1467, 2013.

[3] A. Muheem et al., "A review on the strategies for oral delivery of proteins and peptides and their clinical perspectives," Saudi Pharmaceutical Journal, vol. 24, no. 4, pp. 413-428, 2016/07/01/ 2016.

[4] P. M. Anderson, D. C. Hanson, D. E. Hasz, M. R. Halet, B. R. Blazar, and A. C. Ochoa, "Cytokines in liposomes: Preliminary studies with IL-1, IL-2, IL-6, GM-CSF and interferon-γ," Cytokine, vol. 6, no. 1, pp. 92-101, 1994.

[5] A. Weiner, "Liposomes for Protein Delivery: Selecting Manufacturing and Development Processes," Immunomethods, vol. 4, pp. 201-209, 1994.

[6] M. Diwan and T. G. Park, "Pegylation enhances protein stability during encapsulation in PLGA microspheres," Journal of Controlled Release, vol. 73, no. 2-3, pp. 233-244, 2001.

[7] S. E. Paramonov et al., "Fully Acid-Degradable Biocompatible Polyacetal Microparticles for Drug Delivery," Bioconjugate Chemistry, vol. 19, no. 4, pp. 911-919, 2008.

[8] N. Murthy, M. Xu, S. Schuck, J. Kunisawa, N. Shastri, and J. M. J. Frechet, "A macromolecular delivery vehicle for protein-based vaccines: Acid-degradable protein-loaded microgels," Proceedings of the National Academy of Sciences, vol. 100, no. 9, pp. 4995-5000, 2003.

[9] S. Allen, O. Osorio, Y. G. Liu, and E. Scott, "Facile assembly and loading of theranostic polymersomes via multi-impingement flash nanoprecipitation," Journal of Controlled Release, vol. 262, no. March, pp. 91-103, 2017.

[10] U. Bilati, E. Allémann, and E. Doelker, "Development of a nanoprecipitation method intended for the entrapment of hydrophilic drugs into nanoparticles," European Journal of Pharmaceutical Sciences, vol. 24, no. 1, pp. 67-75, 2005.

[11] U. Bilati and E. Doelker, "Nanoprecipitation Versus Emulsion-based Techniques for the Encapsulation of Proteins Into Biodegradable Nanoparticles and Process-related Stability Issues," AAPS PharmSciTech, vol. 6, no. 4, pp. 594-604, 2005.

[12] R. F. Pagels and R. K. Prud'homme, "Polymeric nanoparticles and microparticles for the delivery of peptides, biologics, and soluble therapeutics," Journal of Controlled Release, vol. 219, no. Supplement C, pp. 519-535, 2015/12/10/ 2015.

[13] C. E. Markwalter and R. K. Prud'homme, "Design of a Small-Scale Multi-Inlet Vortex Mixer for Scalable Nanoparticle Production and Application to the Encapsulation of Biologics by Inverse Flash NanoPrecipitation," Journal of pharmaceutical sciences, 2018.

[14] Y. Liu, C. Y. Cheng, R. K. Prud'homme, and R. O. Fox, "Mixing in a multi-inlet vortex mixer (MIVM) for flash nano-precipitation," Chemical Engineering Science, vol. 63, no. 11, pp. 2829-2842, Jun 2008.

[15] B. K. Johnson and R. K. Prud'homme, "Chemical processing and micromixing in confined impinging jets," AIChE Journal, vol. 49, no. 9, pp. 2264-2282, 2003.

[16] J. Feng, C. E. Markwalter, C. Tian, M. Armstrong, and R. K. Prud'homme, "Translational formulation of nanoparticle therapeutics from laboratory discovery to clinical scale," Journal of translational medicine, vol. 17, no. 1, p. 200, 2019.

[17] C. E. Markwalter, R. F. Pagels, B. K. Wilson, K. D. Ristroph, and R. K. Prud'homme, "Flash nanoprecipitation for the encapsulation of hydrophobic and hydrophilic compounds in polymeric nanoparticles," JoVE (Journal of Visualized Experiments), no. 143, p. e58757, 2019.

[18] C. E. Markwalter, R. F. Pagels, A. N. Hejazi, A. G. R. Gordon, A. I. Thompson, and R. K. Prud'homme, "Polymeric nanocarrier formulations of biologics using inverse Flash NanoPrecipitation," AAPS Journal, vol. 22, no. 18, 2020.

[19] A. Alexander, S. Ajazuddin, D. Tripathi, T. Verma, J. Mayura, and S. Patel, "Mechanism responsible for mucoadhesion of mucoadhesive drug delivery system: a review," International journal of applied biology and pharmaceutical technology, vol. 2, no. 1, pp. 434-445, 2011.

[20] B. M. Boddupalli, Z. N. Mohammed, R. A. Nath, and D. Banji, "Mucoadhesive drug delivery system: An overview," Journal of advanced pharmaceutical technology & research, vol. 1, no. 4, p. 381, 2010.

[21] M. Yang et al., "Biodegradable nanoparticles composed entirely of safe materials that rapidly penetrate human mucus," Angewandte Chemie, vol. 123, no. 11, pp. 2645-2648, 2011.

[22] L. M. Ensign, C. Schneider, J. S. Suk, R. Cone, and J. Hanes, "Mucus penetrating nanoparticles: biophysical tool and method of drug and gene delivery," Advanced Materials, vol. 24, no. 28, pp. 3887-3894, 2012.

[23] R. F. Pagels, J. Edelstein, C. Tang, and R. K. Prud'homme, "Controlling and Predicting Nanoparticle Formation by Block Copolymer Directed Rapid Precipitations," Nano Letters, vol. 18, no. 2, pp. 1139-1144, Feb 2018.

[24] R. F. Pagels and R. K. Prud'homme, "Inverse Flash NanoPrecipitation for Biologics Encapsulation: Nanoparticle Formation and Ionic Stabilization in Organic Solvents," in Control of Amphiphile Self-Assembling at the Molecular Level: Supra-Molecular Assemblies with Tuned Physicochemical Properties for Delivery Applications, vol. 1271(ACS Symposium Series, no. 1271): American Chemical Society, 2017, pp. 249-274.

[25] C. E. Markwalter and R. K. Prud'homme, "Inverse Flash NanoPrecipitation for Biologics Encapsulation: Understanding Process Losses via an Extraction Protocol," in Control of Amphiphile Self-Assembling at the Molecular Level: Supra-Molecular Assemblies with Tuned Physicochemical Properties for Delivery Applications, vol. 1271(ACS Symposium Series, no. 1271): American Chemical Society, 2017, pp. 275-296.

[26] N. M. Pinkerton et al., "Single-Step Assembly of Multimodal Imaging Nanocarriers: MRI and Long-Wavelength Fluorescence Imaging," Advanced healthcare materials, vol. 4, no. 9, pp. 1376-1385, 2015.

[27] J. Feng, C. E. Markwalter, C. Tian, M. Armstrong, and R. K. Prud'homme, "Translational formulation of nanoparticle therapeutics from laboratory discovery to clinical scale," Journal of Translational Medicine, vol. 17, Jun 2019, Art. no. 200.

[28] J. Feng et al., "Amorphous nanoparticles by self-assembly: processing for controlled release of hydrophobic molecules," Soft matter, vol. 15, no. 11, pp. 2400-2410, 2019.

[29] J. Feng et al., "Rapid Recovery of Clofazimine-Loaded Nanoparticles with Long-Term Storage Stability as Anti-Cryptosporidium Therapy," ACS applied nano materials, vol. 1, no. 5, pp. 2184-2194, 2018 May 25 (Epub 2018 Apr 2018.

Prnano.com, https://doi.org/10.33218/001c.18519 Andover House, Andover, MA USA
The official Journal of CLINAM – ISSN:2639-9431 (online)

Supporting Information

Table S1: NC size and PDI for Figure 1B

Name	Size (nm)	PDI
NC1	48.6 ± 2.1	0.21
NC2	73.9 ± 1.5	0.19
NC3	81.7 ± 1.7	0.19

Table S2: NC size and PDI for Figure 1C

Name	Size (nm)	PDI
NC1	149.5 ± 94.1	0.43
NC2	77.4 ± 15.6	0.34
NC3	75.8 ± 8.2	0.30

Table S3: NC size and PDI for Figure 2

Process	Size (nm)	PDI
Extract with brine	120.3 ± 3.2	0.13
Extract with PBS	115.7 ± 2.2	0.13
Solvent swap with THF	129.4 ± 3.0	0.16
Solvent swap with acetone	1275.7 ± 202	0.60

Table S4: NC size and PDI for Figure 3

Components	Size (nm)	PDI
iNCs in THF	134.2 ± 4.0	0.16
iNCs/HPMCAS	321.9 ± 5.9	0.18
HPMCAS only	222.9 ± 7.9	0.17
iNCs only	214.1 ± 4.8	0.27

Prnano.com, https://doi.org/10.33218/001c.18519
The official Journal of CLINAM – ISSN:2639-9431 (online)
Andover House, Andover, MA USA

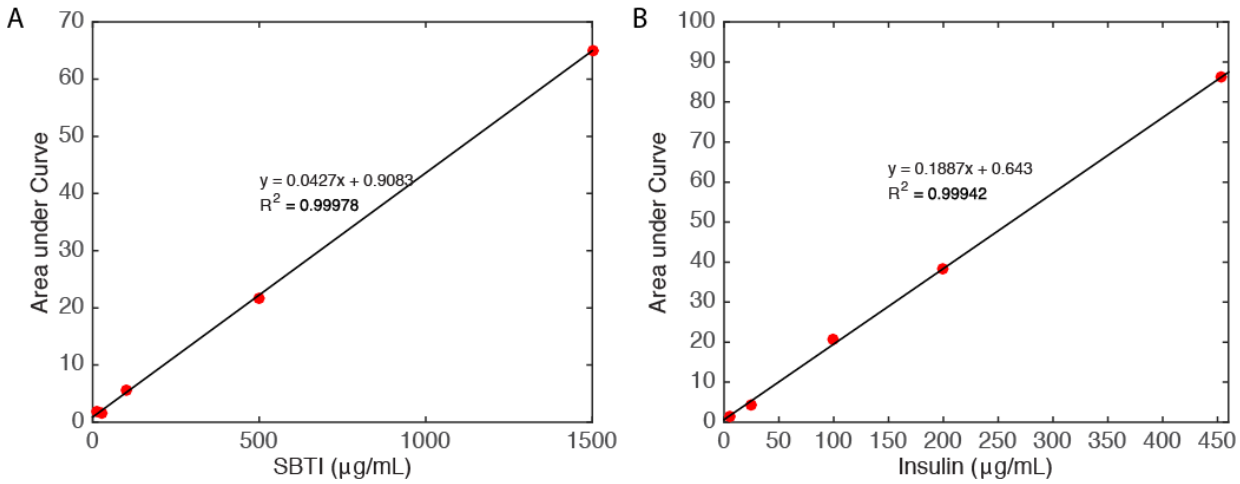

Figure S1: Standard Curves for (A) SBTI and (B) insulin from integration of the main peaks on HPLC.

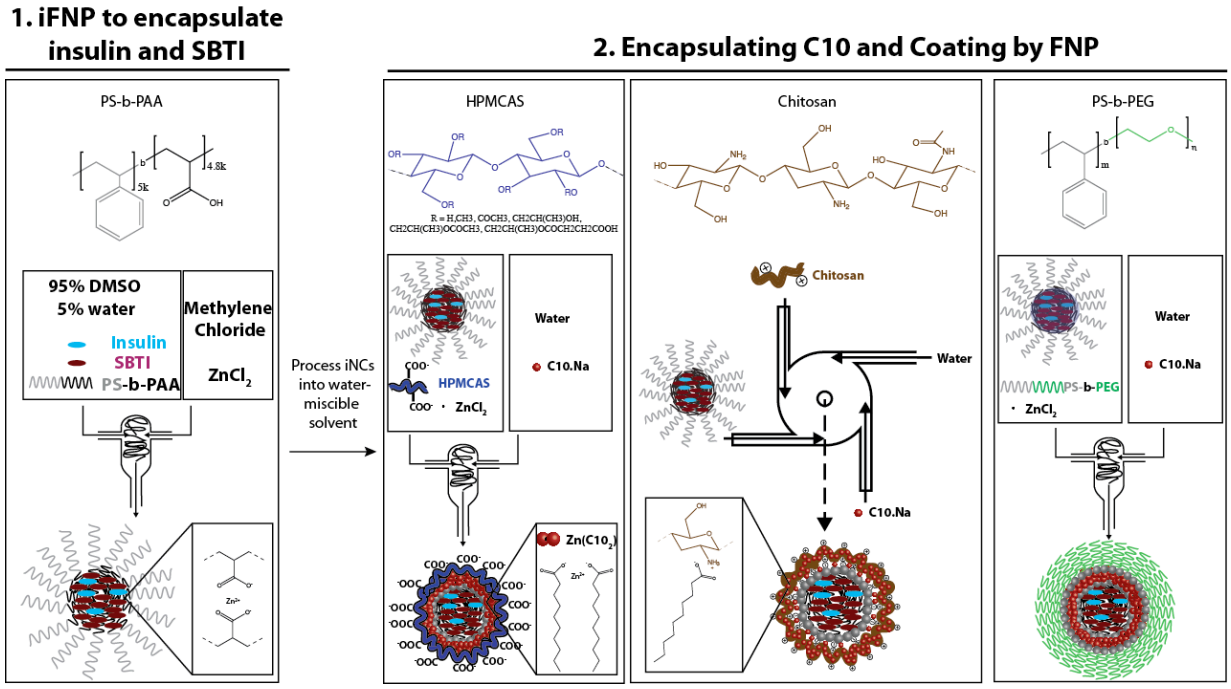

Figure S2: Encapsulation of insulin, SBTI, and sodium caprate into NCs. 1. Inverse Flash NanoPrecipitation (iFNP) to encapsulate insulin, and SBTI. 2. Flash NanoPrecipitation (FNP) to encapsulate sodium caprate and coat with HPMCAS, chitosan, or PS-b-PEG.

Prnano.com, https://doi.org/10.33218/001c.18519
The official Journal of CLINAM – ISSN:2639-9431 (online)
Andover House, Andover, MA USA

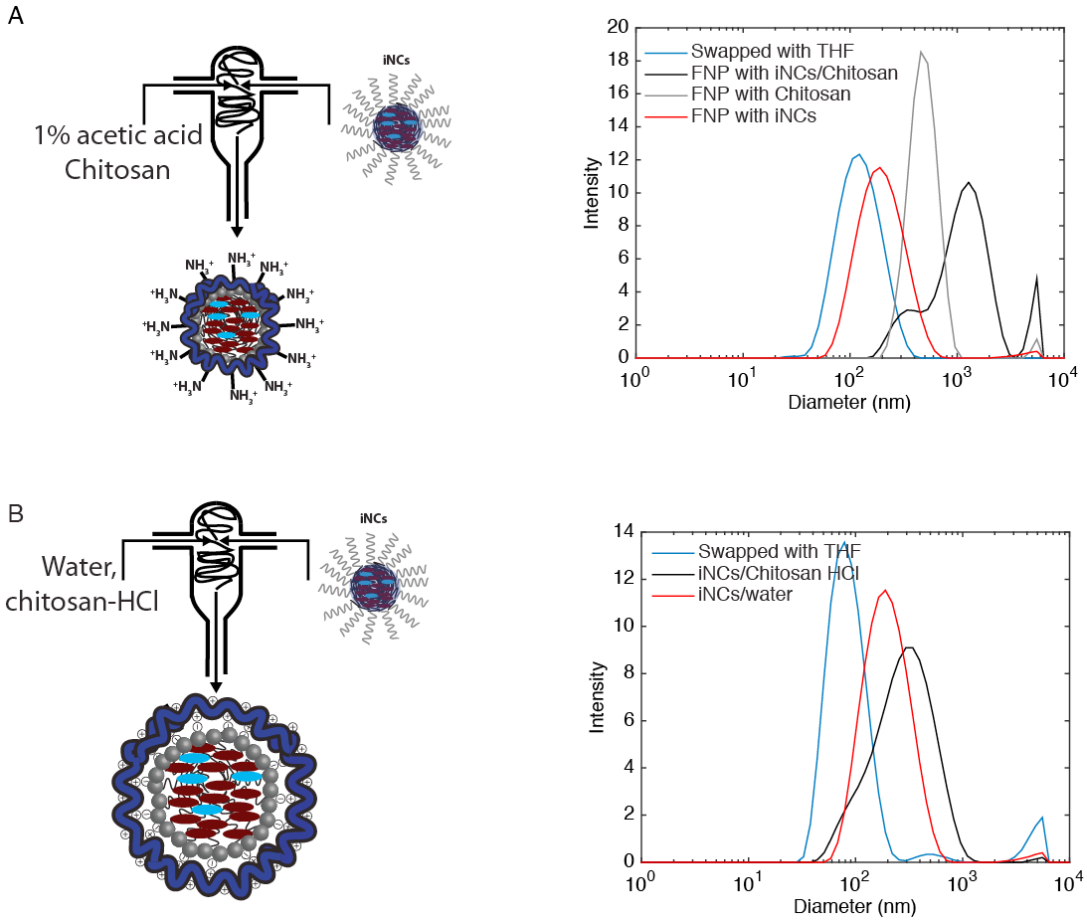

Figure S3: Coating iNCs with chitosan and chitosan-HCl. (A) chitosan coated from a 1% acetic acid and chitosan NCs showed significant aggregation. (B) The more highly charged, chitosan-HCl produced cationic, chitosan coated NCs in FNP process.

Table S5. NC size and PDI for **Figure S3A**.

Components	Sizes (nm)	PDI
iNCs/THF	132.7 ± 1.0	0.16
iNCs/chitosan	1254 ± 192	0.56
chitosan only	491.6 ± 93.6	0.25
iNPs only	160.5 ± 4.0	0.27

Prnano.com, https://doi.org/10.33218/001c.18519
The official Journal of CLINAM – ISSN:2639-9431 (online)
Andover House, Andover, MA USA

Table S6: NC size and PDI for **Figure S3B**.

Components	Size (nm)	PDI
iNCs/Chitosan-HCl	320.7 ± 16.6	0.28
iNCs only	160.5 ± 4.0	0.27
iNCs/THF	87.1 ± 4.3	0.28

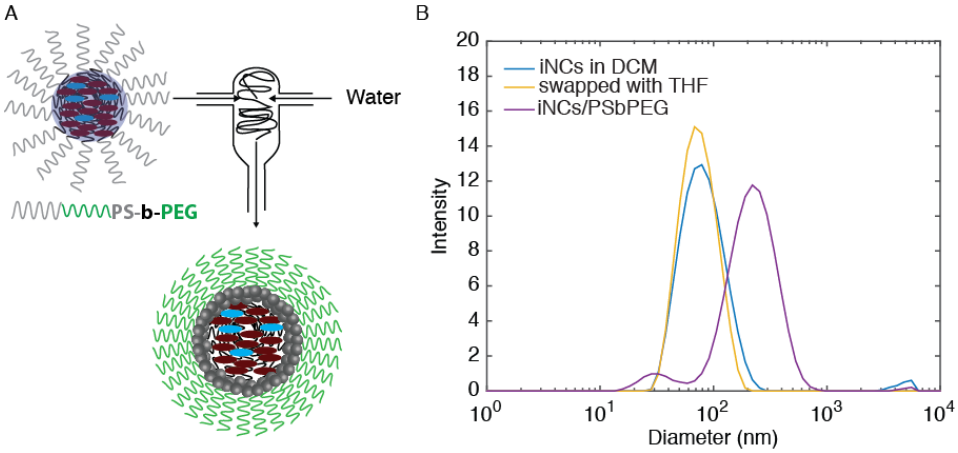

Figure S4: iNC coating with PS-b-PEG. (A) iNCs swapped into THF were coated with PS-b-PEG in a second FNP step. (B) The size distributions of the iNCs in DCM, transferred to THF, and coated with PS-b-PEG are shown.

Table S7. NC size and PDI for **Figure S4B**

Components	Size (nm)	PDI
iNCs in DCM	87.6 ± 4.0	0.19
iNCs in THF	81.2 ± 7.7	0.21
iNCs, PS-b-PEG	171.9 ± 7.7	0.56

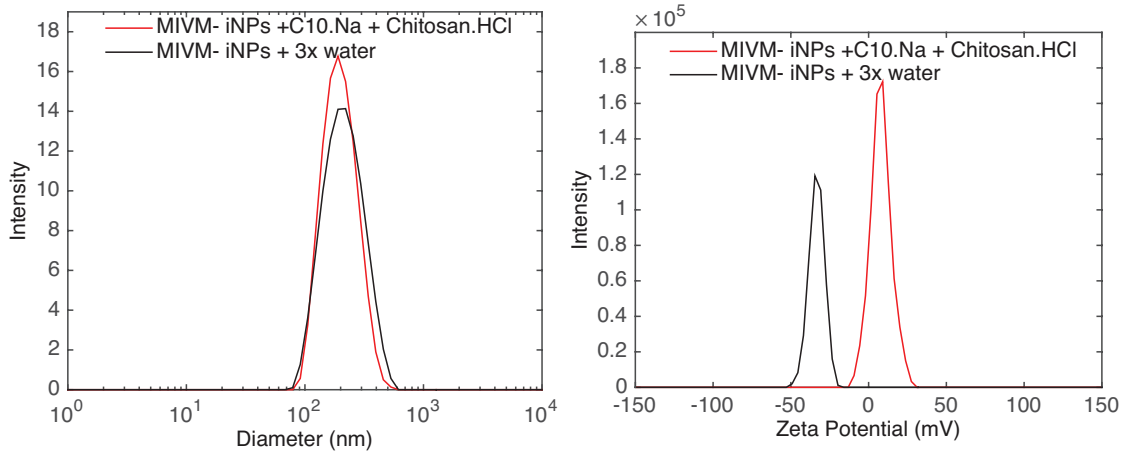

Prnano.com, https://doi.org/10.33218/001c.18519
The official Journal of CLINAM – ISSN:2639-9431 (online)
Andover House, Andover, MA USA

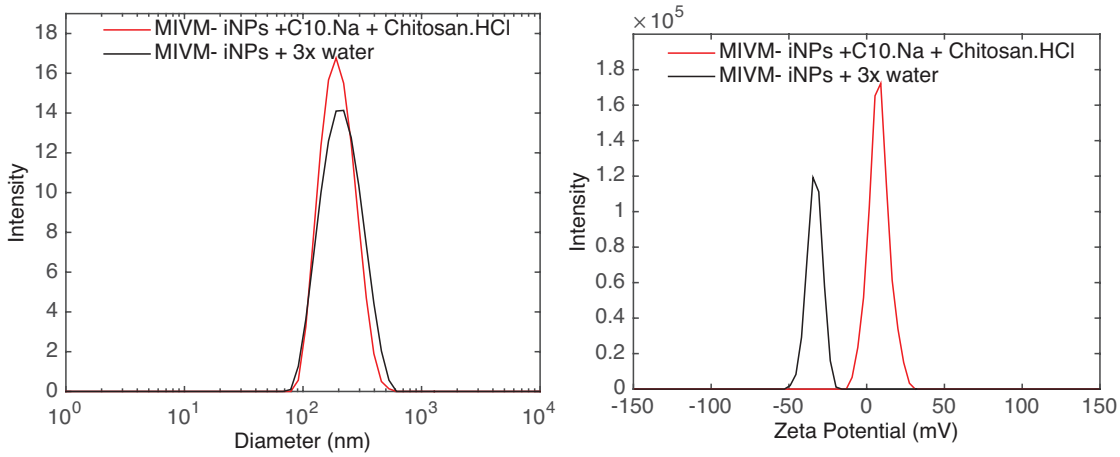

Figure S5: Figure S4: DLS and zeta potential of chitosan:NaC10 coated iNCs and uncoated iNCs (MIVM against 3 streams of water). Both particles give similar size distributions. Uncoated NCs gave a negative zeta potential, (-30 mV) associated with some exposure of the inner acrylic acid polymer block on the iNC surface, since a second coating layer of polymer was not applied. The chitosan:NaC10 coated NCs gave a positive zeta potential (+8 mV). While some of the chitosan cationic groups were involved in complexing the anionic C10 acid, sufficient cationic charge was available to give the iNCs a net cationic charge.

Prnano.com, https://doi.org/10.33218/001c.18519
The official Journal of CLINAM – ISSN:2639-9431 (online)
Andover House, Andover, MA USA